Solar Radio Burst and Solar Wind Associations with Inferred Near-Relativistic Electron Injections

S. W. Kahler
Air Force Research Laboratory, Space Vehicles Directorate, 29 Randolph Rd., Hanscom AFB, MA 01731

H. Aurass and G. Mann
Astrophysikalisches Institut Potsdam, An der Sternwarte 16a, D-14482 Potsdam, Germany
and

A. Klassen
Institut für Experimentelle und Angewandte Physik, Universität Kiel, Leibnizstrasse 11, D-24118 Kiel, Germany

ABSTRACT

The solar injections of near-relativistic (NR) electrons observed at 1 AU appear to be systematically delayed by $\sim$ 10 min from the associated flare impulsive phases. We compare inferred injection times of 80 electron events observed by the 3DP electron detector on the *Wind* spacecraft with 40-800 MHz solar observations by the AIP radio telescope in Tremsdorf, Germany. Other than preceding type III bursts, we find no single radio signature characteristic of the inferred electron injection times. The injection delays do not correlate with the 1 AU solar wind β_p or B, but do correlate weakly with densities n_e and inversely with speeds V_{SW}, consistent with propagation effects. About half the events are associated with metric or decametric-hectometric (dh) type II bursts, but most injections occur before or after those bursts. Electron events with long ($\geq$ 2 hr) beaming times at 1 AU are preferentially associated with type II bursts, which supports the possibility of a class of shock-accelerated NR electron events.

Subject headings: acceleration of particles - interplanetary medium - Sun: particle emission - Sun: radio radiation - Sun: coronal mass ejections

1. Introduction

The acceleration of near-relativistic (NR, $E >$ 30 keV) electrons in the solar corona and their injection into space has been a subject of recent controversy. Early observations of 2–100 keV electron events at 1 AU suggested that impulsive acceleration occurs in solar flares accompanied by fast-drift metric and/or decametric type III radio bursts (Lin 1985) produced by beams of escaping electrons. However, recent results, based on observations of NR electron events by the Electron, Proton, and Alpha Monitor (EPAM) on the *ACE* spacecraft (Haggerty & Roelof 2002; Haggerty, Roelof, & Simnett 2003) and by the 3-D Plasma and Energetic Particle (3DP) experiment on the *Wind* spacecraft (Krucker et al. 1999) at 1 AU, have indicated that in most events the solar injections are delayed from the type III burst times by up to half an hour.

Recent work has focussed on comparisons of solar electron injection times with corresponding coronal EUV, white light, and radio signatures to determine how the electron acceleration occurs. Krucker et al. (1999), Klassen et al. (2002), and

Simnett, Roelof, & Haggerty (2002) have argued for acceleration in coronal shocks. The inferred injections occur when the shocks, often producing type II radio bursts, or the coronal mass ejection (CME) shock drivers reach heights of $\sim$ 1.5–4 $R_\odot$ from Sun center.

Kahler et al. (2005) looked for coronal shock associations of 100 $E \geq 25$ keV electron events (discussed in § 2) observed with the *Wind* 3DP instrument. Those electron events were compared with metric type II (hereafter type IIm) bursts observed by the Tremsdorf radiospectrograph of the Astrophysikalisches Institut Potsdam (AIP), decametric-hectometric type II (hereafter type IIdh) bursts observed by the *Wind*/WAVES instrument, and CMEs observed by the *SOHO*/LASCO coronagraph. Only event associations were examined; the detailed relationships of the burst or CME times to inferred electron injection times were not considered. The associations of the electron events with type IIm (37%) and type IIdh (17%) bursts were not high, suggesting that most electron events do not originate in shocks. The 80% CME association was higher, but the consideration that shocks are driven only by wide ($> 60°$) and fast (> 900 km s^{-1}) CMEs (Gopalswamy et al. 2001) suggested an $\sim 50\%$ association of the electron events with fast and wide CMEs. Kahler et al. (2005) concluded that at least some, and perhaps most, NR electron events are not associated with coronal shocks.

Studies comparing inferred NR electron injections with metric radio coronal imaging observations from the Nancay Radioheliograph (NRH) have provided an alternative acceleration explanation for some events. Maia & Pick (2004) discussed 18 EPAM events (Haggerty & Roelof 2002), of which 7 were consistent with injections during relatively simple radio signatures of type III bursts only. Injections of 6 of the 11 radio-complex events occurred during NRH continuum emission consistent with acceleration and release of electrons during coronal magnetic reconnection, but not in CME-driven shocks. While shock acceleration could not be excluded in the 5 cases of radio-complex events with type II bursts, Maia & Pick (2004) suggested shock-induced magnetic reconnection as the principal acceleration scenario.

A similar result was based on a survey of 40 3DP events (Klein et al. 2005), of which 10 showed no emission in the NRH frequency range of 164-432 MHz. In 18 of 30 cases with observed emission the inferred injection windows were in or close to a short group of bursts, and in 12 of those 18 cases they were consistent with no delays from the first radio signatures of energetic electrons. In the 12 cases of injections during long (> 10 minutes) periods of observed metric radio emission the relationships between injection and radio emission were complex, but the injections were always associated with new increases in radio emission. Although type II bursts were associated with at least 15 of the 30 NRH radio events and CMEs with 19 of the 26 NRH events with LASCO observations, Klein et al. (2005) argued that in most such cases the delayed electron injections were better matched to accelerations of radio-emitting electrons at heights lower than those of the shocks. They favored post-eruptive magnetic reconnection as the sources of the NR electrons, similar to the conclusions of Maia & Pick (2004).

All the NR electron events observed at 1 AU are associated with dh type III bursts (Haggerty & Roelof 2002) which, at least for the events with delayed injections, are presumed to have no direct relevance to those electron events. A very different interpretation was suggested by Cane (2003), who found that the inferred injection delay times of 79 EPAM electron events correlated directly with the times for the radio-generating electrons to transit to 1 AU. In addition, a correlation of the delays was also found with the 1 AU ambient solar wind densities, leading her to conclude that interaction effects in the interplanetary medium were the cause of the inferred anomalous delays of the electron event onsets. This implies that the basic assumption that the first-arriving NR electrons propagate scatter-free, used to infer the electron solar injection times, is not valid. In this case there is only a single population of energetic electrons producing both the type III radio bursts and the events at 1 AU.

In this work we compare in detail a set of 80 3DP NR ($E > 25$ keV) electron events with metric radiospectrographic observations of the AIP Tremsdorf Observatory and with solar wind parameters. These events are a subset of the 100 events used by Kahler et al. (2005) in a survey of the associations of NR electron events with type II bursts and with CMEs, as summarized above

in the discussion of the possible shock origin of the electrons. After confirming the inferred injection delays from type III burst times, we examine in detail some of the properties of the electron events, their associated metric and decimetric radio bursts, and associated solar wind parameters. Our goal here is to use all the events of a large statistical data sample to understand the solar origins of the NR electron events at 1 AU. We look for correlations of the electron injection times with solar radio bursts and compare the injection delays with solar radio and solar wind characteristics.

2. Data Analysis

2.1. Selection of the NR 3DP Electron Events

The selection of the 3DP NR electron events for analysis was based on two previous event listings: (1) the electron events from the *Wind* 3DP solid state telescope (SST) ranked as "mediocre" and "good" at the web site http://sprg.ssl.berkeley.edu /∼bezerkly/, and (2) the beamed events observed in the highest energy channels of the *ACE* EPAM instrument, given in Table 2 of Haggerty & Roelof (2002) and extended through the end of 2001 (D. Haggerty, private communication). AIP Tremsdorf radio observations from about 1 hour before each inferred electron injection time through that injection time and *Wind*/WAVES 20 kHz to 14 MHz observations through the event durations were required. Kahler et al. (2005) discussed the detailed selection criteria for the 100 events, of which we here use the subset of 80 events given in Table 1.

Along with Krucker et al. (1999) and Haggerty & Roelof (2002) we assume that the first observed electrons of each event have propagated scatter-free to 1 AU following a simultaneous solar injection at all electron energies. The event onset times were estimated by eye from the intensity-time profiles of the 3DP SST. Solar injection times were derived from the apparent onset times of the 3DP 66-135 keV channel, using an effective electron energy and $v_e/c = \beta$ of 82 keV and 0.507, respectively, with magnetic field path lengths calculated from the ambient solar wind speeds at times of onsets. The net result is that we subtracted 9 to 13 minutes from the 82 keV electron onset times at 1 AU to get the injection times relative to the observed solar radio times; the injection times are given in column 2 of Table 1. All events of the study showed strong pitch-angle anisotropy and velocity dispersion in their onsets. We did not attempt to do $1/\beta$ (Krucker et al. 1999) fits to derive the electron injection times. We find that the injection times of 14 of the 16 events of Table 1 in common with the 30 3DP events of the Klein et al. (2005) study lay within their $\sim$ 6 to 10 minute injection time intervals, indicating good agreement with their injection determinations. In addition, our injection times differ by an average of only 2 minutes from those of the 13 EPAM electron events in common with the study of Maia & Pick (2004). Thus the determination of the electron injection times by different techniques appears to give consistent results (Haggerty & Roelof 2002).

2.2. The Injection Delay Times

We generated high-time resolution plots of WAVES radio emission in the 350 to 10^7 Hz range for the periods around the electron injection times. An associated *Wind* WAVES type IIIdh burst was found for all the electron events of Table 1 except that of 2000 March 6, for which there is a WAVES data gap. The highest frequency at which the burst could be observed in the WAVES plots, F_{max}, and the start and end times of the burst at F_{max} are given in columns 5 and 4, respectively. We examined background-subtracted AIP radiospectrograms for 40-800 MHz type IIIm bursts associated with those WAVES bursts and give in column 3 the onset and qualitative assessments of the relative intensities (strong, moderate, or weak) of the most intense component of each burst. In 17 cases there was no type IIIm burst preceding the injection by up to $\sim$ 30-40 minutes. Figures 1 through 4 show examples of the AIP and WAVES radio spectra and the 3DP SST counting rate profiles.

The delay times between the inferred solar electron injections and the 63 associated type IIIm burst start times ranged from –2 to 53 minutes, with a median of 12 minutes. We expect the event delay times relative to the type IIIdh bursts to be frequency dependent, decreasing with lower F_{max} as the dh emission drifts to lower frequencies at later times. Selecting only the 57 WAVES type IIIdh bursts with $F_{max} \geq 3$ MHz, we find simi-

lar delay times of –1 to 55 minutes, with a median of 12 minutes. We also ask whether those delay times depend on the intensities of the electron events, such that onsets of more intense electron events are observed earlier due to their higher signal-to-noise (S/N) ratios in the 3DP detector. S/N ratios of the 3DP 82 keV electron channel background-subtracted peak counting rates to the pre-event background rates are given in column 8 of Table 1. No correlation between the event delay times and their S/N ratios was found.

Another electron event parameter we measured was the approximate time over which the event pitch-angle distribution (PAD) remained highly anisotropic, indicating a clear beaming of electrons antisunward. These times, given in column 7 of Table 1, ranged from 0.2 to 7 hours, based on qualitative assessments of color-coded PADs of the 3DP channel 3 shown in grey scales in the top panels of Figures 1 to 4. In 6 cases, indicated as NA, the 3DP plot did not include enough of the PAD at 0° and 180° to make a good determination of the beaming time. While we expect these beaming times to depend on the interplanetary scattering of the electrons, we also take these times as probable indicators of the solar electron injection durations.

We looked for flare associations for all the events of Table 1 and were able to make associations for the 59 events shown in column 12. The locations were determined on the basis of Hα flare reports and X-ray and EUV images from the *Yohkoh* SXT and *SOHO* EIT instruments, respectively. We could not determine possible flare locations for the remaining 21 events. The flare locations are generally magnetically well connected to the Earth. Eleven are at or over the west limb (WL). Of the 4 flares located in the eastern hemisphere two (18 December 1997 and 20 October 2002) are not associated with GOES X-ray flares and may not be true associations. We used the solar wind speeds of column 10 to calculate the longitudinal angular displacements of the Earth magnetic footpoints from the solar flare sites, setting the WL longitudes to be W100°. We found no dependence on flare longitudinal separation for the delay times from either the type IIIm bursts (46 cases) or from the type IIIdh bursts with $F_{max} \geq$ 3 MHz (41 cases).

2.3. Event Comparisons with Type III, Type II, and Decimetric Bursts

The 63 electron events of Table 1 with associated type IIIm bursts are compared with those burst intensities at the top of Table 2. We also separate out the 21 events with the shortest delay times ($\leq$ 8 minutes; see Figures 1,2 and 4) and the 20 events with the longest delay times ($\geq$ 17 minutes; see Figure 3) to look for any association differences between those groups. We find only a slight tendency for the short-delay events to be associated with strong type IIIm bursts; otherwise the delay times show no dependence on the type IIIm burst intensities.

Many of the electron events were associated with type II bursts. We compare the 80 event injection times with those burst times in the middle of Table 2. The type IIm burst start and end times were taken from the AIP plots and those of type IIdh from the WAVES list at http://lep694.gsfc.nasa.gov/waves/waves.html. There were 31 and 15 events associated with type IIm and type IIdh bursts, respectively, and their relative injection times are shown in column 6 of Table 1. Table 2 shows that the injection times for most (23 of 31) of the type IIm and about half (7 of 15) the type IIdh associated cases did not occur during the type II bursts themselves, but occurred either before or after them, as seen in the examples of Figures 2 and 3. As we should expect, the injections with short (long) delay times from the type IIIm bursts are more likely to occur before (after) the times of the type II bursts. Thus, only 8 of the 80 electron injections occurred during type IIm bursts and another 8 during type IIdh bursts (Table 2).

Decimetric emission at $f > 200$ MHz was examined in the AIP radiospectrograms to look for evidence of energetic electron production in the lower corona. If decimetric emission was present within $\pm$ 2 minutes of the inferred injection time, we give the burst classification in column 9 of Table 1 as the high-frequency component of a type IIIm burst (III) or as a burst of new emission (Y), probably an extension of a microwave or metric type IV burst. Otherwise, there was no emission (N), a data gap (NA), or only an earlier $f > 200$ MHz component of the associated preceding metric type III burst (IIIpc). The distributions are given at the bottom

of Table 2 for the injection times of the 80 electron events. In only 23 (18 burst and 5 type III) of the 73 events with available observations do we find simultaneous decimetric emission. The distributions of the short and long delay groups are not significantly different from the entire group.

2.4. Delay Time Comparisons with Ambient Solar Wind Parameters

Following the work of Cane (2003), we compare the inferred injection delay times with ambient solar wind parameters measured at 1 AU. In columns 10 and 11 of Table 1 we list the solar wind speeds V_{SW} and the logs of the plasma β_p values computed from *Wind* measurements of n_e and B. Both the associated 63 type IIIm and the 57 type IIIdh delay times are weakly negatively correlated with V_{SW} at $r \sim 0.3$ and a 99% confidence level (Figure 5). However, neither group of delay times are significantly correlated with the logs of β_p or with B. We do find weak correlations at $r \sim 0.4$ (99% confidence level) between the delay times and n_e only when we delete two outlier events with high delay times (1995 October 19) and with a high n_e (2000 March 19).

2.5. Anisotropic PAD Durations

The injection delay times are not correlated with the PAD beaming durations. However, we do find that the events with the longest ($\geq$ 2 hours) beaming durations are well associated with the presence of m/dh type II bursts, in contrast to those with the shortest ($\leq$ 0.3 hours; see Figure 1) durations, as indicated in Table 3. We do not find significant correlations of the beaming durations with any of the solar wind parameters of V_{SW}, β_p, B, or n_e. This suggests that the extended electron beaming times reflect the durations of the injections rather than the particle transport properties. This may mean two kinds of solar injection, one impulsive at well connected flare sites and the other extended at broad CME-driven shocks.

We can test this idea by looking at the longitudinal displacements of the associated flares from longitudes of Earth connection. The median flare longitudinal displacement of the 13 long-duration beamed events associated with flares is 26°, somewhat wider than the 15° of the 10 short-duration beamed events. However, comparing more broadly the flare locations of the No type II events of Table 1, assumed to be impulsive flare injections, with those of the m/dh type II bursts, assumed to be shock injections, we find comparable median flare displacements of 26° for the 29 No type II events and 29° for the 30 m/dh type II events. Thus while the flare longitude displacements provide some support for impulsive flare and extended shock injection for the shortest and longest injections, respectively, such a distinction between the two kinds of suggested electron injections for all events is not obvious based on these simple event associations with type II bursts.

3. Discussion

3.1. Interpretation of the Injection Delay Times

We have selected 80 3DP NR electron events for a statistical study to determine the solar conditions of their injections. In each case we determined an onset of the solar injection time based on the 82 keV electron onset at the 3DP and the assumption of scatter-free propagation. Similar event surveys (e.g., Klein et al. 2005, Maia & Pick 2004) have further selected for detailed comparison only those events with significant associated solar radio bursts during the injection times. Complex or long-duration ($\geq$ 10 minutes) metric radio bursts were associated with 11 of the 21 electron events of Maia & Pick (2004) and 12 of the 40 electron events of Klein et al. (2005). Remaining events had either short duration emission, typically type III bursts, or no emission in the metric/decametric range. Thus, the interpretation of the solar acceleration and injection conditions has been focussed on bursts which are not representative of all observed NR electron events. We have indicated in Table 1 which electron events have been included in other detailed studies; the 2000 February 18 event in particular has been been analyzed in the works of four different groups. Our goal here is to describe all 80 electron events statistically.

We confirm the electron injection delay times found by others. Our median time for delays from the type IIIm bursts is 12 minutes, and the times range from –2 to 55 minutes, although only one event exceeded 39 minutes. Delays from the type IIIdh bursts are similar. The Hα flare locations

and their longitudinal footpoint displacements do not order the delay times, as Haggerty et al. (2003, their Figure 1) found. Further, the delay times do not depend on the peak intensities of the electron events themselves or on the intensities of the associated type IIIm bursts (Table 2).

We used the AIP radiospectrograms to examine the associations of the injections with type II bursts and with other decimetric emission. Only 31 and 15 of the 80 events were associated with metric and dh type II bursts, respectively, suggesting that shocks were not the sources of the majority of events. On the other hand, about half of the events with the longest (≥ 17 minutes) delay times were associated with type II bursts, suggesting that some electron events could have had delayed injections from type II shocks, even though the inferred injections often occurred before or after the burst times. An examination of the decimetric emissions (Table 2) indicates that only 18 of 73 (25%) injection times occurred during emissions other than accompanying or preceding type III bursts. These 18 events may correspond to the group of long-duration or complex bursts selected for detailed study in the metric range by Klein et al. (2005) and Maia & Pick (2004). We do not find a significant difference between the short and long delay events in these associations. In general we find a lack of any consistent signature other than the presence of preceding type III bursts for the events of the study.

If the electron injection delays are due to interaction effects in the interplanetary medium, as argued by Cane (2003), then the delay times should scale with the electron travel distances to 1 AU. To test this requirement, we did compare the delay times with V_{SW} and found the weak inverse correlation shown in Figure 5, consistent with a scaling with travel distance. Cane (2003) favored a single population of energetic electrons producing both the type III radio bursts and the NR electron events at 1 AU. Haggerty & Roelof (2002) used the type III burst drift rates between the 14 and 2 MHz peak intensities to argue that the burst excitor speeds were $\sim c/12$, corresponding to electrons of ~ 2 keV that constitute a population separate from the NR population. However, Mann & Klassen (2005) make clear that the electron beams producing type III bursts evolve in space and time so that different parts of the electron distributions are responsible for the type III burst radiation at different locations (i.e., frequencies) during their coronal propagation. Thus, contrary to the Haggerty & Roelof (2002) argument, NR electrons could be injected in type III bursts.

We looked for further evidence that the electron injection delay times may be correlated with solar wind properties. Because of the general inverse correlation between in situ particle anisotropies and solar wind β_p (Crooker et al. 2003) we compared the injection delay times with β_p, as well as with solar wind B and n_p. We found correlations of delay times with n_p, a result also found by Cane (2003), but no correlations with β_p or with B. Because all the NR electron events are preceded by type IIIdh bursts, and the delay times correlate with the type III drift times to 1 AU and with n_e (Cane 2003) and inversely with V_{SW} (Fig. 5), the idea that the delays are due to propagation effects deserves serious consideration.

3.2. Multiple Classes of NR Electron Events

We are dealing with two interrelated questions in this analysis. The first is to determine whether there are indeed apparent injection delays from the times of the accompanying type III bursts, and if so, how long those delays are. The inferred solar injection times may be correct as most workers assume, or some or all times may be incorrectly inferred to be delayed due to propagation effects, as Cane (2003) suggested. The second problem is then to determine the acceleration mechanism(s) by associating the injection times with solar radio bursts, with the understanding that the inferred delays may be spurious.

We used rough estimates of the event PAD anisotropy durations as guides to injection durations. We first established that the anisotropy durations are not correlated with the solar wind β_p, a possibility suggested by the results of Crooker et al. (2003). We separated out two event groups of long and short-duration PAD anisotropies to compare with type II bursts with the idea that electrons of the long-duration group are injected over longer times and larger spatial regions from shocks and that electrons of the short-duration group may be injected only over the short intervals of the type III bursts from well connected source regions. The result in Table 3 supports

this suggestion with, of course, limited statistics. The longitudinal footpoint displacements of the Hα flares of long-duration beamed events exceeded those of short-duration events by 26° versus 15°. We take these results as weak support for two different kinds of injections, one impulsive, with type III bursts, and the other more extended, from shocks. However, the mere presence of type II bursts may not be a good guide to shock acceleration of electrons, as we found comparable longitudinal footpoint displacements for the flares of electron events with and without type II bursts.

If there are two or more kinds of electron acceleration and injection, we might expect to see multi-phase electron profiles in large SEP events. The well studied 2003 October 28 NR electron event is a good candidate. It had an impulsive component with an injection delayed by 11 minutes from the type III burst and was followed by a gradual component with a harder spectrum and delayed by 25 minutes from the type III burst (Klassen et al. 2005). Besides the low-energy ($\leq$ 30 keV) electrons of the intense type III burst, Klassen et al. (2005) note that the impulsive component injection occurred during decimetric/metric type II and type IV bursts, so it could be attributed to either shock or coronal magnetic field reconfigurations. They consider that the gradual component is more likely attributable to magnetic reconfiguration behind the shock. The properties of the impulsive electron component suggested to Simnett (2005a) an impulsive injection of electrons accelerated in a CME-driven shock when the halo CME reached $\sim$ 5 R$\odot$. For the source of the gradual electron component, which had a harder spectrum and a longer time scale, he suggested that electrons produced at the flare site were trapped in the propagating CME. Those electrons gradually leaked out and were significantly backscattered beyond 1 AU to account for their observed weak anisotropy. A challenge for the October 28 event is to understand how the electrons can be observed at Earth from such a poorly connected (S16E08) flare region. Miroshnichenko et al.(2005) noted that the dominant 164 MHz source during the type III bursts lay in the western hemisphere, well away from AR 10486 at E08. They suggested that the impulsive electrons were injected from the well connected western source region which also produced the earlier type III radio emission, but the gradual component electrons were injected from the flare site into the eastern footpoint of an ICME loop at 1 AU. Although they differed on the details, all these authors interpreted the October 28 electron event as at least two separate electron injections from different sources and/or acceleration mechanisms. This interpretation is consistent with Lin's (1985) two electron groups of (1) impulsive 2-100 keV events with single power-law energy spectra from small flares and (2) long-lived $E > 20$ keV events with broken power-law spectra from large flares. The significant difference is that his group (1) events were injected during the type III bursts, and the recent interpretations delay those injections to after the type III bursts.

3.3. Diagnostics for Multiple NR and Relativistic Electron Events

Are there two or more kinds of NR electron events? The basic paradigm for SEP ion events is that there are impulsive and gradual events (i.e., Reames 1999), the former produced near flaring active regions and the latter in CME-driven shocks. Our understanding of the two kinds of ion events has evolved from studies of their very different elemental abundances, ionic charge states, solar source longitude ranges, peak intensities and flare/CME associations. The possible bases for distinguishing two (or more) kinds or sources of electron events appear to be limited to the electron event spectra, their timescales, and the solar phenomena associated with the times of electron injections. The NR speeds of the electrons are favorable for fixing their solar injection times, but a systematic delay due to interplanetary scattering could yield seriously misleading injection associations with relevant solar events. In particular, it may suggest a low-energy electron population producing the type III bursts but rarely detected at 1 AU and a second population from a delayed injection (i.e., Haggerty et al. 2003), when in fact the two populations could be one (Cane 2003). On the other hand, the spectra and timescales could serve to contrast two classes (Lin 1985). As an example, Simnett & Roelof (2005) attributed the electron event of 2005 January 20 to the associated well connected flare, rather than to the associated fast (> 2500 km s^{-1}) CME, because of the hard electron spectrum and long event duration.

Relativistic ($E > 0.3$ MeV) electron injection delays from CME limb times were studied by Stolpovskii et al. (1997). They found that the delays increased substantially outside a longitudinal footpoint separation range of $\pm$ 30° for electron events observed on the *Helios* spacecraft. A model of shock propagation at the observed CME speed away from the flare site to the magnetic field line connected to *Helios* gave good agreement with the observed injection delays. In addition, the electron intensity rise times, measured from event onsets to peak intensities and normalized to 1 AU, correlated with CME speeds. A correlation between CME speed and harder electron spectra has now been found for both NR (Simnett et al. 2002, Haggerty et al. 2003) and relativistic (Stolpovskii et al. 2001) electron events. In the latter case a spectral softening with increasing longitudinal separations from CME longitudes was also found. These delay, rise-phase, and spectral results suggest that CME-driven shock acceleration plays a major role in the production of relativistic electron events.

CME associations with flares are more likely with increasing soft X-ray flare durations (Sheeley et al. 1983, Andrews 2003), so differences between electron events associated with short ($\leq$ 1 hr, SDE) or long ($>$ 1 hr, LDE) duration flares may be additional evidence of at least two different electron acceleration mechanisms. Kahler et al. (1994), comparing the *Helios* $E > 0.3$ MeV electron events with flare durations and locations, found shorter ($<$ 2 hr) electron event rise times for SDE and longitudinally well connected ($\leq 20°$) associated flares. In a complementary study Moses et al. (1989) compared X-ray flare durations to 0.75 keV $< E <$ 100 MeV electron event spectra measured by detectors on *ISEE* 3. Plotting spectra in units of number density per momentum versus rigidity (momentum), they found broken power-law spectra associated exclusively with SDEs. The relatively soft, single power-law spectra were associated with LDEs. Moses et al. (1989) preferred to interpret the two kinds of spectra in terms of differences in coronal heights and densities for electron acceleration, but allowed for the possibility of shock acceleration of electrons in the LDEs and, by implication, two classes of electron events.

There are clearly many relativistic (Stolpovskii et al. 2001) and NR (Kahler et al. 2005) electron events that are not associated with CMEs. Also, most NR electron events are not associated with m/dh type II bursts (Kahler et al. 2005). Those events are therefore not likely to be produced in coronal shocks. Recently Simnett (2005b) has identified a sequence of 9 NR EPAM electron events observed during a quiet solar period with no apparent flare or CME associations and only low frequency ($\leq$ 10 MHz) associated type III radio bursts. Those electron events are characterized by short durations of $\sim$ 30 minutes, and very soft energy spectra that extend to $\sim$ 200 keV. This appears to define a class of electrons of coronal origin but not produced in either flares or CME-driven shocks. The current observations therefore suggest at least two classes of electron events extending over both the NR and relativistic energy ranges. One of these classes is probably due to shock acceleration. There may well be three or more classes of events in the NR range. We are currently limited in our diagnostic techniques to sorting out the spectra, time scales and solar X-ray and radio phenomena of the source region. However, we must first understand the nature of the anomalous delays before we proceed to a comprehensive classification of events with their defining physical characteristics, appropriate diagnostics, and solar sources.

3.4. Acknowledgments

We thank S. Krucker for his help and advice with access to the 3DP software, D. Haggerty for the EPAM event list, and H. Cane for sharing her event flare associations with us. SK thanks the AIP for their hospitality and the Air Force Office of Scientific Research for funding his Window on Europe visit to the AIP. The AIP acknowledges the European Office for Aerospace Research and Development for its support in maintaining the solar radio spectral observations at Potsdam.

TABLE 1

SOLAR NR ELECTRON EVENTS AND ASSOCIATED FLARE RADIO AND SOLAR WIND OBSERVATIONS

Date	Electron Injec. UT	Metric III UT/int.[a]	WAVES III UT	WAVES F_{max}	Type II injection[b]	PAD dur.[c]	S/N	decim emis.[d]	V_{SW} km/s	LOG β_p	Flare Site
1995											
06 Mar	0847	0826/md	0821-0830	10	A m/N dh	4	4.67	N	442	– 0.9	S15W58
02 Apr	0843	none	0830-0835	1	N II	0.2	1.33	N	360	– 0.41	S13W54
02 Apr	1112	1107/wk	1106-1108	10	N II	0.4	56.2	N	365	– 0.45	S15W54
02 Apr	1432	1423/wk	1420-1423	3	N II	0.3	8.3	IIIpc	352	– 0.48	S15W58
19 Oct	1122	1029/wk	1027-1030	10	N II	1.6	5.3	Y	415	– 2.15	S14W45
1996											
01 Jul	1305	1234/md	1249-1257	0.8	A m/N dh	2	7	IIIpc	340	– 0.18	N08W83
09 Jul	0802	0751/wk	0753-0758	3	N II	1.4	3.71	Y	425	NA	S11W23
09 Jul	0924	0912/stg	0910-0914	4	A m/N dh	1.5	53.8	Y	420	NA	S11W30
14 Jul	1505	1446/stg	1445-1449	10	N II	0.3	9	IIIpc	378	NA	S10W90
13 Aug	1551	none	1510-1516	1	A m/N dh	NA	7.5	N	370	– 0.05	
24 Dec	1316[e]	1306/wk	1305-1310	10	D m/N dh	1.2	50	IIIpc	373	– 0.8	N05W93
1997											
07 Apr	1419	1401/stg	1356-1410	10	A m/B dh	1	100	Y	405	– 0.15	S29E20
12 May	0517	0457/md	0458-0503	10	A m/D dh	1	90	Y	305	– 0.05	N21W08
27 May	1026	0956/wk	0954-0958	10	N II	0.5	142.9	IIIpc	320	– 0.88	N02W76
07 Oct	1326	none	1251-1256	1	A m/N dh	6	50	N	335	0.21	SWL
06 Nov	1224[e]	1154/stg	1153-1157	10	A m/D dh	3.5	25	Y	350	0.24	S18W63
18 Dec	1229	none	1203-1207	2	N II	1.5	5	IIIpc	300	– 0.39	N19E08
1998											
20 Apr	1029[ef]	1007/wk	1008-1030	1	A m/D dh	6	438	Y	370	– 0.36	S43W90
02 May	0500	0455/stg	0455-0508	10	N II	2	5.6	III	630	– 1.2	S20W10
02 May	1345[e]	1337/stg	1338-1344	10	D m/B dh	5	5.4	Y	600	– 1.68	S15W15
06 May	0801	0803/stg	0802-0807	10	B m/B dh	3	60	IIIpc	465	– 2.02	S15W64
27 May	1325[e]	1320/stg	1315-1325	10	N m/B dh	0.5	116.7	Y	470	0.1	N18W60
15 Jun	0639	none	0610-0630	0.3	N II	0.5	1.4	Y	380	– 0.58	S25W90
16 Jun	1901[f]	(1822)/md	1826-1842	1	A m/D dh	NA	1.6	NA	400	– 1.08	S20W90
22 Jun	0452	none	0433-0443	2	A m/N dh	1.5	3	N	400	NA	N15W46
13 Aug	1513	1508/stg	1505-1508	10	N II	3	2.3	IIIpc	360	– 1.61	
14 Aug	0606	0557/md	0556-0600	10	N II	0.5	5.4	IIIpc	385	– 0.37	S23W73
06 Sep	0612	0558/wk	0551-0557	2	N II	0.5	2.1	Y	355	– 0.02	N30W90
08 Sep	1528	1522/stg	1521-1525	10	N II	0.3	8	N	350	– 1.57	
27 Sep	0816[e]	0809/stg	0805-0812	10	N II	0.3	42.9	III	540	– 0.18	N21W48
30 Sep	1343[eg]	none	1325-1333	10	A m/D dh	3	23.1	Y	420	– 0.45	N20W84
05 Nov	1347	1335/stg	1332-1340	10	N II	0.3	2.8	IIIpc	410	0.05	N15W17
1999											
24 Jan	1125	none	1112-1130	0.6	N II	0.2	2.1	N	525	0.18	N21W30
20 Feb	1516	∼1513/stg	1511-1518	10	N II	0.3	42.5	N	425	– 1.8	S17W71
21 Feb	0951	0943/stg	0945-0949	10	B m/N dh	NA	80	III	380	– 1.18	
24 Apr	1330	1312/wk	1300-1322	1	N m/B dh	0.2	15	Y	430	0.16	NWL
08 May	1442[eg]	1425/stg	1424-1427	10	B m/N dh	NA	2.7	Y	415	– 0.74	N23W75
12 May	0658	0654/md	0654-0657	10	N II	0.2	4.4	IIIpc	470	– 1.52	
27 May	1057[eg]	(1052)/md	1051-1056	10	A m/D dh	1.2	76.9	IIIpc	455	– 0.44	WL
31 May	0956[eg]	0937/stg	0935-0940	10	A m/N dh	2	4.5	IIIpc	360	– 0.94	N18W27
13 Jun	0526	0517/wk	0515-0518	10	N II	1.5	2.5	N	375	– 0.48	
18 Jun	0728	0711/md	0712-0715	3	N II	1	4.9	III	390	– 0.36	
18 Jun	1143	1129/md	1129-1132	10	N II	1	8	III	380	– 0.22	
18 Jun	1438	1424/md	1423-1427	10	N II	1	8	IIIpc	380	– 0.23	
18 Jun	1657	1641/stg	1638-1644	10	A m/N dh	1	3.3	IIIpc	375	– 0.15	

TABLE 1—*Continued*

Date	Electron Injec. UT	Metric III UT/int.[a]	WAVES III UT	WAVES F_{max}	Type II injection[b]	PAD dur.[c]	S/N	decim emis.[d]	V_{SW} km/s	LOG β_p	Flare Site
23 Jun	0605	0544/wk	0541-0545	10	A m/D dh	2	7.9	IIIpc	310	– 0.53	
16 Jul	1604	1552/wk	1552-1556	10	D m/N dh	0.5	20	IIIpc	350	– 0.21	NWL
20 Jul	0841	0819/md	0818-0821	6	N II	NA	2.5	IIIpc	290	– 0.07	S12W70
27 Oct	0924	0910/stg	0908-0915	10	D m/N dh	1	8.8	IIIpc	395	– 0.36	S12W15
2000											
18 Feb	0927[efgh]	none	0925-0928	2	D m/N dh	2.5	33.3	NA	400	– 0.86	NWL
02 Mar	0838[g]	0825/stg	0824-0829	10	A m/N dh	1.7	10	NA	435	– 0.51	S14W52
06 Mar	1221[e]	1211/md	Data Gap	DG	N II	1.5	3.3	IIIpc	435	– 0.45	
07 Mar	0736	0724/md	0724-0727	10	N II	1	10	NA	440	– 0.6	
07 Mar	1237	1229/wk	1229-1233	10	N II	0.7	23.3	NA	440	– 0.64	S11W14
07 Mar	1518[e]	1512/wk	1512-1516	10	N II	0.3	2.9	NA	435	– 0.61	
19 Mar	1304	1245/wk	1244-1248	10	N II	NA	16.7	NA	355	1.29	
04 Apr	1520[g]	1518/stg	1517-1522	10	B m/N dh	0.8	350	Y	380	– 0.4	N16W66
19 Apr	1238[e]	1231/stg	1229-1233	10	N II	1.5	2	IIIpc	430	– 0.49	
27 Apr	1425	none	1416-1423	1	N II	0.7	3.8	N	410	– 0.3	N32W90
2001											
30 Apr	1057[e]	1058/wk	1057-1059	10	N II	0.4	11.4	IIIpc	440	– 1.82	N30WL
2002											
20 Feb	1114	1106/stg	1104-1109	10	N II	1	2.5	IIIpc	390	– 0.72	N15W77
25 Feb	1217	1205/wk	1204-1206	10	N II	0.2	3	N	360	NA	S01W51
27 Feb	1211	1158/md	1157-1200	5	N II	1	3	IIIpc	345	– 0.62	N23W15
22 Mar	1109	1049/wk	1049-1051	10	D m/B dh	1.2	5	N	440	– 0.22	S10WL
27 Mar	1457	1441/wk	1439-1444	5	N II	0.3	11.8	N	480	– 0.22	
28 Mar	0839	0823/wk	0821-0824	5	N II	0.5	12	N	380	– 0.2	S25WL
11 Apr	1629	1618/wk	1618-1624	10	D m/N dh	3	66.7	IIIpc	468	– 0.58	S15W33
15 Apr	1752	(none)	1725-1735	1	N II	0.8	8.8	N	359	– 0.4	S16W60
20 May	1546	1525/stg	1524-1533	10	A m/N dh	0.4	3	IIIpc	446	– 1.05	S21E65
30 May	0522	0518/wk	0457-0509	0.5	N II	2.5	17.5	Y	514	– 0.03	N10WL
02 Jun	1026[i]	(none)	1014-1017	10	D m/N dh	0.4	11.1	Y	399	– 0.03	S20W61
30 Jun	0922	none	0900-0910	1	N II	0.7	2.7	Y	367	– 0.2	
07 Jul	1149	1115/md	1117-1125	1	N m/D dh	7	20	IIIpc	423	– 0.45	
03 Aug	1335	(none)	1324-1327	10	N II	0.4	1.9	N	442	– 0.95	
16 Aug	0609	(none)	0557-0601	4	N m/B dh	1.1	59.1	N	577	– 0.2	N07W83
24 Sep	1118	none	1115-1121	0.5	N II	1.4	12	N	366	NA	S05WL
24 Sep	1133	1131/wk	1132-1142	0.5	N II	”	13.3	N	366	NA	S05WL
26 Sep	1234	none	1221-1230	1	N II	0.4	4	N	345	NA	
20 Oct	1145	1135/wk	1136-1140	1	N II	0.2	2.5	N	664	– 0.63	N25E55
20 Oct	1418	1412/md	1411-1414	5	B m/N dh	0.8	50	N	649	– 0.52	S13W63

[a]Metric type III burst UT onset times and relative intensities [stg, strong; md, moderate; wk, weak].

[b]Electron injection times relative to AIP metric (m) or WAVES decametric-hectometric (dh) type II bursts, if any [A, after; B, before; D, during; N II, no type II burst.

[c]Time in hours during which the PAD plots showed clear beaming.

[d]Observed decimetric (> 200 MHz) emission. N, none; Y(s), (strong) new emission preceding electron injection; III, extension of type III burst only; –, data gap.

[e]Described in Klein et al. (2005).

[f]Described in Klassen et al. (2002).

[g]Described in Maia & Pick (2004).

[h]Described in Haggerty & Roelof (2002) and Simnett et al. (2002).

[i]Described in Classen et al. (2003).

TABLE 2
NR ELECTRON EVENT ASSOCIATIONS WITH AIP METRIC OBSERVATIONS

Burst Type	Burst Descriptor	Short Delay[a]	All 80 Events	Long Delay[b]
Type IIIm	Strong	12	23	6
	Moderate	3	16	7
	Weak	6	24	7
	None	N.A.	17	N.A.
Type IIm	Before	4	5	1
	During	1	8	1
	After	1	18	10
	None	15	49	8
Type IIdh	Before	3	7	3
	During	1	8	6
	After	0	0	0
	None	17	65	11
Decimetric	Y	4	18	7
	III	3	5	1
	IIIpc	7	27	8
	N	5	23	2
	N.A.	2	7	2

[a]Total 21 events with delays $\leq$ 8 minutes

[b]Total 20 events with delays $\geq$ 17 minutes

TABLE 3
NR ELECTRON BEAMING DURATIONS AND TYPE II BURST ASSOCIATIONS

Type II Burst Descriptor	Short Duration[a]	All 74 Events	Long Duration[b]
m/dh Type II	1	31	13
No Type II	13	43	3

[a]Total 14 events with beam durations ≤ 0.3 hours

[b]Total 16 events with beam durations ≥ 2 hours

REFERENCES

Andrews, M. D. 2003, Solar Phys., 218, 261

Bougeret, J.-L., et al. 1995, Space Sci. Rev., 71, 5

Cane, H. V. 2003, ApJ, 598, 1403

Classen, H. T., Mann, G., Klassen, A., & Aurass, H. 2003, A&A, 409, 309

Crooker, N. U., Larson, D. E., Kahler, S. W., Lamassa, S. M., & Spence, H. E. 2003, Geophys. Res. Lett., 30(12), 21, DOI 10.1029/2003GL017036

Gopalswamy, N., Yashiro, S., Kaiser, M. L., Howard, R. A., & Bougeret, J.-L. 2001, J. Geophys. Res., 106, 29219

Haggerty, D. K., & Roelof, E. C. 2002, ApJ, 579, 841

Haggerty, D. K., Roelof, E. C., & Simnett, G. M. 2003, Adv. Space Res., 32(12), 2673

Kahler, S. W., Stolpovskii, V. G., & Daibog, E. I. 1994, in Solar Coronal Structures, eds. V. Rusin et al., IAU Colloq. 144, 479

Kahler, S. W., Aurass, H., Mann, G., & Klassen, A. 2005, in Coronal and Stellar Mass Ejections, eds. K. P. Dere et al., Proc. IAU Symp. 226, 338

Klassen, A., Bothmer, V., Mann, G., Reiner, M. J., Krucker, S., Vourlidas, A., & Kunow, H. 2002, A&A, 385, 1078

Klassen, A., Krucker, S., Kunow, H., Muller-Mellin, R., Wimmer-Schweingruber, R., Mann, G., & Posner, A. 2005, J. Geophys. Res., 110, A09S04, doi: 10.1029/2004JA010910

Klein, K.-L., Krucker, S., Trottet, G., & Hoang, S. 2005, A&A, 431, 1047

Krucker, S., Larson, D. E., Lin, R. P., & Thompson, B. J. 1999, ApJ, 519, 864

Lin, R. P. 1985, Sol. Phys., 100, 537

Maia, D. J., & Pick, M. 2004, ApJ, 609, 1082

Mann, G., & Klassen, A. 2005, A&A, 441, 319

Miroshnichenko, L. I., Klein, K.-L., Trottet, G., Lantos, P., Vashenyuk, E. V., Balabin, Y. V., & Gvozdevsky, B. B. 2005, J. Geophys. Res., 110, A09S08, doi: 10.1029/2004JA010936

Moses, D., Dröge, W., Meyer, P., & Evenson, P. 1989, ApJ, 346, 523

Poquerusse, M., Hoang, S., Bougeret, J.-L., & Moncuquet, M. 1996, Proc. Eighth Int. Sol. Wind Conf. (eds. D. Winterhalter et al.), AIP Conf Proc. 382, AIP, 62

Reames, D. V. 1999, Space Science Rev., 90, 413

Sheeley, N. R., Jr., Howard, R. A., Koomen, M. J., & Michels, D. J. 1983, ApJ, 272, 349

Simnett, G. M. 2005a, J. Geophys. Res., 110, A09S01, doi: 10.1029/2004JA010789

Simnett, G. M. 2005b, Sol. Phys., 229, 213

Simnett, G. M., Roelof, E. C., & Haggerty, D. K. 2002, ApJ, 579, 854

Simnett, G. M., & Roelof, E. C. 2005, Proc. 29th Int. Cosmic-Ray Conf. (Pune), in press

Stolpovskii, V. G., Daibog, E. I., Svertilov, S. I., Kahler, S. W., & Erdos, G. 1997, Proc. 25th Int. Cosmic-Ray Conf. (Durban), 1, 189

Stolpovskii, V., Daibog, E., Erdös, G., Kahler, S., Kecskeméty, K., & Kunow, H. 2001, Proc. 27th Int. Cosmic-Ray Conf. (Hamburg), 8, 3454

This 2-column preprint was prepared with the AAS LaTeX macros v5.2.

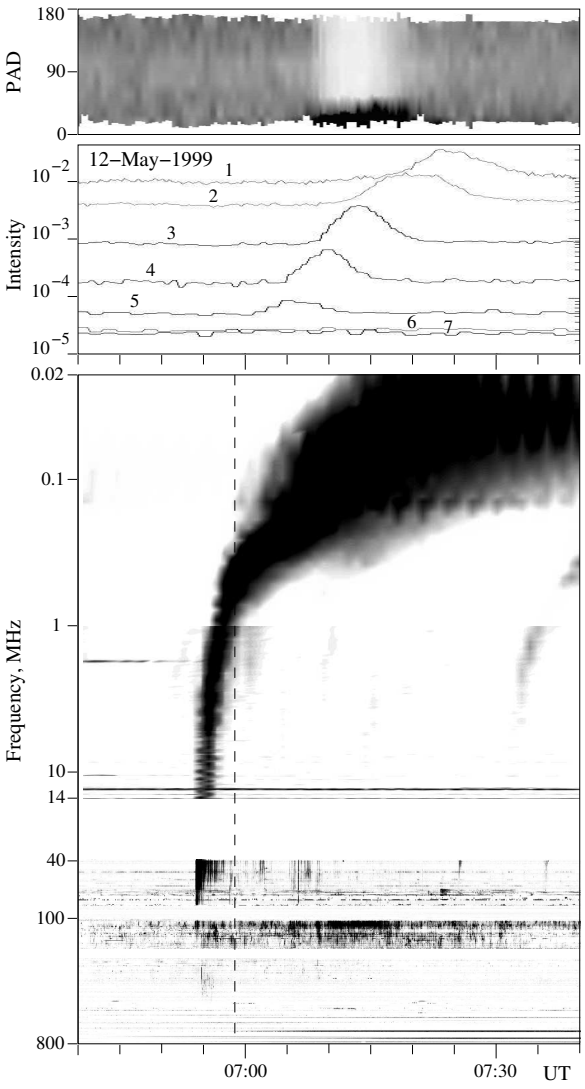

Fig. 1.— The electron event of 1999 May 12. Top panel is the normalized PAD of the 3DP channel 3, corresponding to an average energy of $\sim$ 82 keV. Middle panel shows the counting rate profiles of 3DP SST channels 1 through 7 covering the energy range $\sim$ 25 to $\sim$ 500 keV. Bottom panel is a composite profile of radio emission from 20 kHz to 14 MHz (*Wind*/WAVES) and 40 to 800 MHz (AIP Tremsdorf). The vertical dashed line indicates the inferred solar electron injection time based on the onset time of the channel 3 counting rates of $\sim$ 82 keV electrons; the injection time is advanced 500 seconds to match the radio emission profile. This electron event had no associated type II burst, a short $\sim$ 0.2 hr PAD beaming time, and a short 4 minute injection delay time.

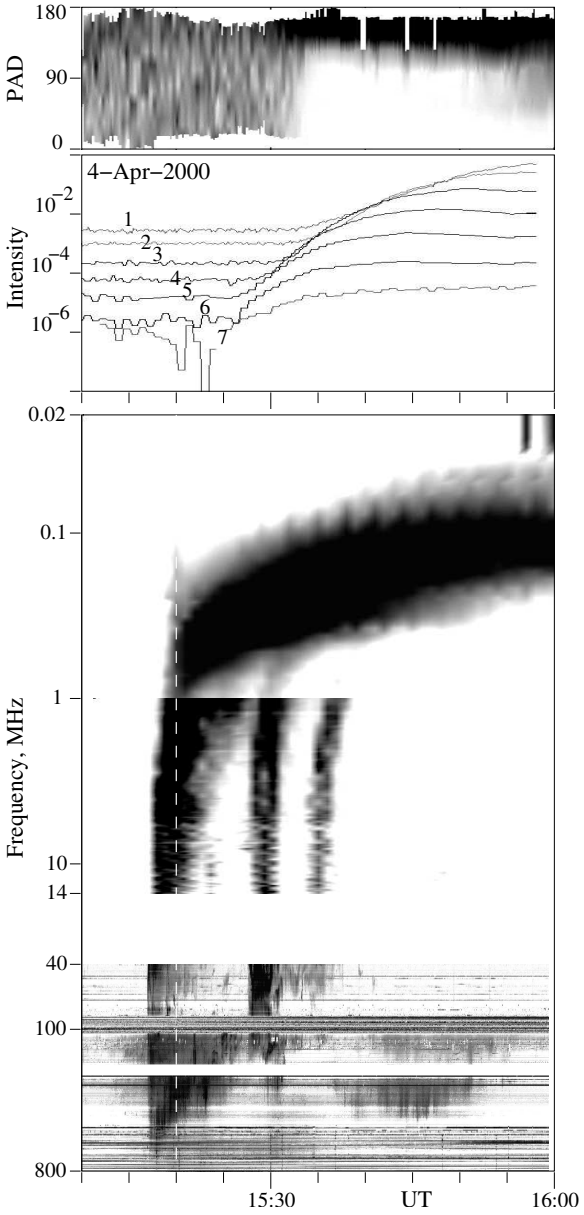

Fig. 2.— The electron event of 2000 April 4. The panel formats are the same as in Figure 1. The inferred solar injection occurred before the 1524.8 UT onset of a short type IIm burst but during a time of significant decimetric emission. The electron injection delay of 2 minutes is one of the shortest of the 80 study events.

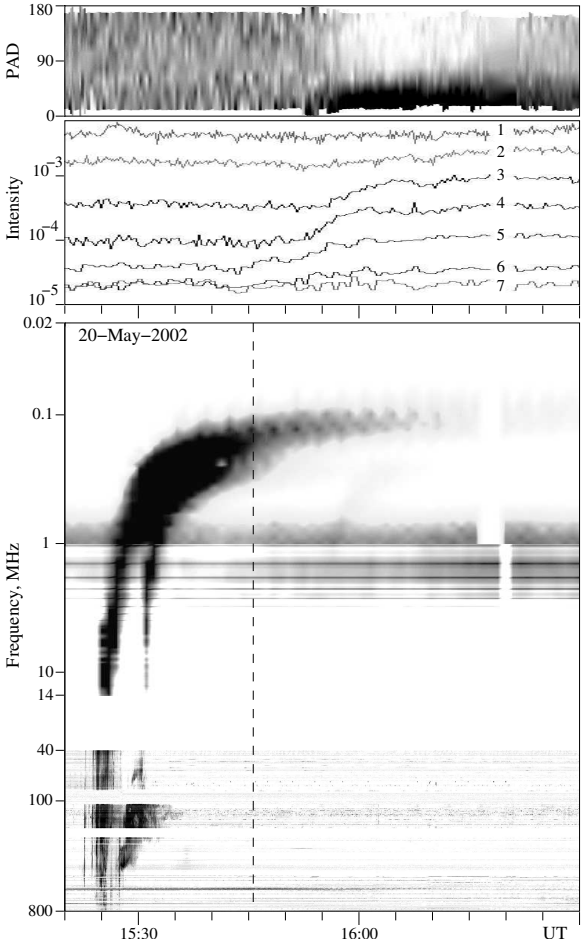

Fig. 3.— The electron event of 2002 May 20. The panel formats are the same as in Figure 1. The inferred electron injection occurred well after the type IIm burst, which ended at 1532 UT. This event has a long ($\geq$ 17 minutes) electron injection delay and is one of 4 associated with an eastern hemisphere flare.

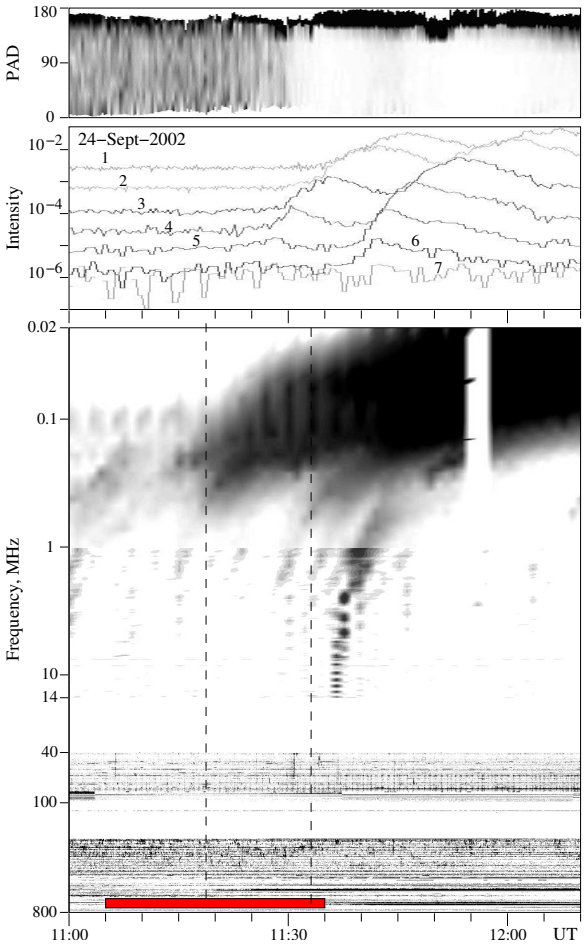

Fig. 4.— The two electron events of 2002 September 24. The panel formats are the same as in Figure 1. The m/dh type III bursts were weak in both events. There was no type II or decimetric emission associated with either injection.

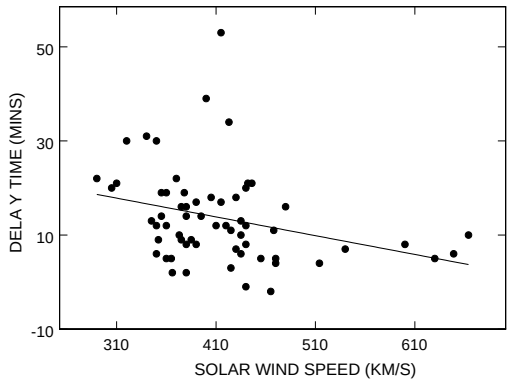

Fig. 5.— The correlation of the 63 delay times from the type IIIm bursts versus the V_{SW} measured at *Wind*. The line shows the least-squares best fit to the data. The correlation coefficient r = 0.31.